Experimental Cosserat elasticity in open cell polymer foam

Zach Rueger and Roderic S. Lakes
Department of Engineering Physics, Engineering Mechanics Program
Department of Materials Science, Rheology Research Center,
University of Wisconsin, 1500 Engineering Drive, Madison, WI 53706-1687

May 25, 2016

Preprint adapted from Philosophical Magazine, 96 (2), 93-111, January (2016).

Abstract

Reticulated open cell polymer foams exhibit substantial size effects in torsion and bending: slender specimens are more rigid than anticipated via classical elasticity. Such size effects are predicted by Cosserat (micropolar) elasticity, which allows points to rotate as well as translate and incorporates distributed moments (couple stresses). The Cosserat characteristic length is larger than the cell size. The Cosserat coupling coefficient is larger than in dense closed cell foams and approaches 1 for foam with 0.4 mm cells.

1 Introduction

Materials that are deformed at sufficiently small strain typically exhibit linear behavior. If the response is also independent of the path of deformation and its time history, the material is considered to be elastic. Classical elasticity is routinely used to model such behavior. There is no length scale in classical elasticity. Length scales do occur in the definition of fracture toughness. Also, toughness of foams is related to the size scale of the cells in the foam [1]. Effects of material length scales may be understood in the context of more general theories of elasticity.

Classical elasticity however is not the only theory of elasticity. Theories that incorporate less freedom or more freedom are available. The Cosserat theory of elasticity [2] [3] incorporates a local rotation of points as well as the translation of classical elasticity, and a couple stress (a torque per unit area) as well as the force stress (force per unit area; just stress in classical elasticity). Eringen [4] incorporated micro-inertia and renamed Cosserat elasticity micropolar elasticity. At frequencies sufficiently low that local resonances are not approached, Cosserat and micropolar are used interchangeably.

The physical origin of the Cosserat couple stress is the summation of bending and twisting moments transmitted by ribs in a foam or by structural elements in other materials (Figure 1). The Cosserat local rotation corresponds to the rotation of ribs. Forces and moments are also considered in the classic analyses of foam by Gibson and Ashby [1] in which classical elastic moduli were determined; effects of rotation gradients were not considered.

The Cosserat theory of elasticity is a *continuum* theory that entails a type of nonlocal [5] interaction. The stress σ_{jk} (force per unit area) can be asymmetric. The distributed moment from this asymmetry is balanced by a couple stress m_{jk} (a torque per unit area). The antisymmetric

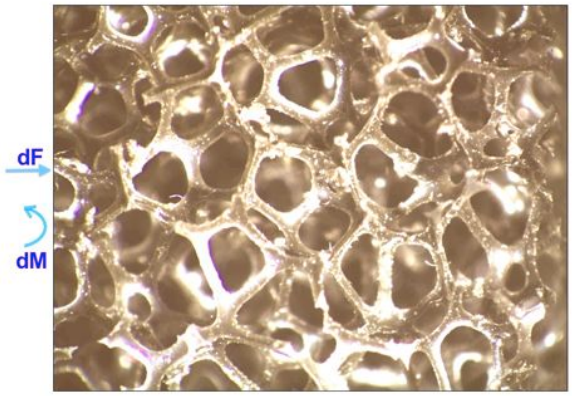

Figure 1: Foam ribs with increment of force dF and increment of moment dM upon ribs.

part of the stress is related to rotations. $\sigma_{jk}^{antisym} = \kappa e_{jkm}(r_m - \phi_m)$ in which κ is an elastic constant, ϕ_m is the rotation of points, called micro-rotation, e_{jkm} is the permutation symbol, and $r_k = \frac{1}{2}e_{klm}u_{m,l}$ is "macro" rotation based on the antisymmetric part of gradient of displacement u_i. The constitutive equations [4] for linear isotropic Cosserat elasticity are as follows.

$$\sigma_{ij} = 2G\epsilon_{ij} + \lambda\epsilon_{kk}\delta_{ij} + \kappa e_{ijk}(r_k - \phi_k) \tag{1}$$

$$m_{ij} = \alpha\phi_{k,k}\delta_{ij} + \beta\phi_{i,j} + \gamma\phi_{j,i} \tag{2}$$

Cosserat elasticity incorporates sensitivity to gradients of rotation by virtue of the coupling between rotations and stresses. It is also possible to supplement classical elasticity with sensitivity to gradients of dilatation [6].

The six isotropic Cosserat elastic constants are as follows in which λ is a Lamé constant from elasticity theory.

$$Young's\ modulus \qquad E = \frac{G(3\lambda + 2G)}{\lambda + G} \tag{3}$$

$$Shear\ modulus \qquad G \tag{4}$$

$$Poisson's\ ratio \qquad \nu = \frac{\lambda}{2(\lambda + G)} \tag{5}$$

$$Characteristic\ length,\ torsion \qquad \ell_t = \sqrt{\frac{\beta + \gamma}{2G}} \tag{6}$$

$$Characteristic\ length,\ bending \qquad \ell_b = \sqrt{\frac{\gamma}{4G}} \tag{7}$$

$$Coupling\ number \qquad N = \sqrt{\frac{\kappa}{2G + \kappa}} \tag{8}$$

$$Polar\ ratio \qquad \Psi = \frac{\beta + \gamma}{\alpha + \beta + \gamma}. \tag{9}$$

Cosserat elasticity has the following consequences. A size effect is predicted in the torsion [7] and bending [8] of circular cylinders of Cosserat elastic materials. Slender cylinders appear more

stiff than expected classically. A similar size effect is also predicted in the bending of plates. No size effect is predicted in tension or compression. The stress concentration factor for a circular hole is smaller than the classical value, and small holes exhibit less stress concentration than larger ones [9]. By contrast, in classical elastic solids, there is no size effect in torsion or bending; structural rigidity goes as the fourth power of the radius; too, stress concentration is independent of hole size.

As for freedom of theories, the early uniconstant elasticity theory of Navier [10] has less freedom than classical elasticity; it has only one elastic constant and Poisson's ratio must be $\frac{1}{4}$ for all materials. This theory is based upon the assumption that forces act along the lines joining pairs of atoms and are proportional to changes in distance between them. This theory was abandoned based on *experiments* that disclosed a range of Poisson's ratio. Classical elasticity has two independent elastic constants for isotropic materials; the Poisson's ratio can have values between -1 and 0.5. Cosserat elasticity has more freedom than classical, that of local rotations and couple stress; there are 6 independent isotropic elastic constants. A simpler variant presented by Koiter [11] assumes that the macrorotation and microrotation vectors are equal. This corresponds to $N = 1$, or equivalently $\kappa \to \infty$ in Cosserat elasticity. The Koiter variant is called couple stress elasticity; there are two characteristic lengths in addition to the classical constants: 4 isotropic elastic constants. The microstructure elasticity theory of Mindlin [12], also called micromorphic elasticity, has more freedom than classical or Cosserat elasticity; it allows points in the continuum to translate, rotate, and deform. This adds considerable complexity; for an isotropic solid, there are 18 micromorphic elastic constants compared with 6 for Cosserat elasticity and 2 for classical elasticity.

Cosserat elastic effects have been observed experimentally. Size effects observed to occur in torsion and bending of closed cell foams [13], [14] and of compact bone [15] are consistent with Cosserat elasticity. The apparent modulus increases substantially as the specimen diameter becomes smaller, in contrast to the predictions of classical elasticity. Cosserat elasticity can account for these observations. For dense (340 kg/m^3) closed cell polyurethane foam [13], $E = 300$ MPa, $G = 104$ MPa, $\nu = 0.4$, $\ell_t = 0.62$ mm, $\ell_b = 0.33$ mm, $N^2 = 0.04$, $\Psi = 1.5$. The cell size ranges from 0.05 mm to 0.15 mm. For dense (380 kg/m^3) polymethacrylamide closed cell foam (Rohacell WF300) [14], $E = 637$ MPa, $G = 285$ MPa, $\ell_t = 0.8$ mm, $\ell_b = 0.77$ mm, $N^2 \approx 0.04$, $\Psi = 1.5$. The cell size is about 0.65 mm. For this material, it was difficult to determine N accurately due to difficulty in cutting sufficiently slender specimens.

The Cosserat characteristic length was determined in a (two dimensional) polymer honeycomb [16]. Full field measurements of deformation reveal non-classical elastic effects that are consistent with Cosserat elasticity. Warp of a bar of rectangular cross section in torsion is predicted to be reduced in a Cosserat elastic solid [17]. The corresponding non-classical strain field was observed in compact bone [18]. Deformation spills over into the corner region where it would be zero in classical elasticity [19] as revealed by holography. This ameliorates concentration of strain. Strain at the corner entails asymmetry of the stress as predicted by Cosserat elasticity. The reduction of warp deformation has been observed via holography [20]. As for plastic deformation, rotational plastic deformation mechanisms were interpreted via gradients in a micropolar continuum theory [21].

The present research deals with experimental study of size effects and Cosserat elasticity in low density open cell polymer foams.

2 Methods

2.1 Materials and experiment

Reticulated polyurethane foam (Scott Industrial foam [22]) was used. One foam had average cell size 1.2 mm or 20 pores per inch (Figure 3); the other foam had average cell size 0.4 mm. For both foams, the density was 30 kg/m^3 so the volume fraction of solid material in the foam was about 0.03.. Separate compression tests on foam cubes were conducted with a servo-hydraulic frame to probe anisotropy.

Cylinders were cut from polymer foam with a hot wire cutter such that the cylinder diameter and length were equal. The wire was Nichrome heater wire of thickness 0.015 inches and resistance 2.5 Ω. The electric current was 3 Amps. The initial cylinder cut from the bulk foam was 45 mm in both diameter and length. The foam cylinder was weighed with an analytical balance, then circular end pieces of the same diameter as the foam specimen were cut from heavy card stock and cemented with cyanoacrylate (Loctite 401) over the full surface. Slight pressure was applied to the end pieces to ensure good adhesion. A catalyst was applied to the surfaces to minimize the amount of cement in order to reduce ingression of the cement into the pores of the smaller cell foam.

These specimens were tested for torsional and bending rigidity using a Broadband Viscoelastic Spectrometer (BVS) [23] [24]. This instrument makes use of a Helmholtz coil acting upon a magnet attached to the specimen to generate torque. The coil spacing is smaller than the larger specimens so a short stalk with a magnet and mirror on the end was fixed to one of the end pieces. A thin aluminum end layer was also cemented to provide a sufficiently rigid attachment for the stalk. First, a small mirror was glued to one face of a cubic magnet. The magnet was then calibrated using the BVS and a lock-in amplifier. The magnetic calibration constants of this particular magnet were obtained by testing a 6061 aluminum alloy rod of known elastic properties; the calibration constants were 8.00 $\times 10^{-6}$ Nm/A in torsion and 1.84 $\times 10^{-5}$ Nm/A in bending. The free end piece of the polymer foam cylinder was cemented to a steel adapter which was screwed in to a 25 mm thick steel rod for holding the specimen inside the BVS. Prior to testing, viscoelastic strain was allowed to recover overnight to enable stable measurements. The specimen (Figure 2, left) was lowered into the BVS such that the magnet was centered in the Helmholtz coils of the BVS. The lower limit on specimen size was imposed by obtrusive presence of incomplete cells, particularly in the larger cell foam; also by difficulty in handling. The smallest specimen of 0.4 mm cell foam is shown in Figure 2, right.

Deformation was measured via a beam from a semiconductor laser reflected from a mirror attached to the magnet that applies torque to the specimen free end. The laser beam was reflected onto a silicon light detector. Prior to torsion tests, the laser based displacement sensor was calibrated. This was done by aligning the laser beam so that the position of the beam on the light detector was centered. The light detector was moved a known amount via a calibrated stage; a calibration curve was obtained via micrometer adjustment. This change in output voltage per change in position was used as the beam position calibration constant (in V/μm).

To test the specimen a sinusoidal signal with a frequency of 1 Hz from a function generator (SRS Model DS345) was input to the torsion Helmholtz coil. Because the same frequency was used for all specimen diameters, viscoelastic effects are decoupled from the size effects to be probed. The torque signal was obtained as the voltage across a 1 ohm resistor in series with the coil to eliminate effects of inductive reactance from the coil. The frequency of 1 Hz was well below any resonant frequencies. The torque signal vs. angular displacement signal was displayed on a digital oscilloscope (Tektronix TDS3014B) using DC coupling. The torque and angle signals were displayed as a Lissajous figure, and used to calculate the modulus and viscoelastic damping of the material. The maximum strain

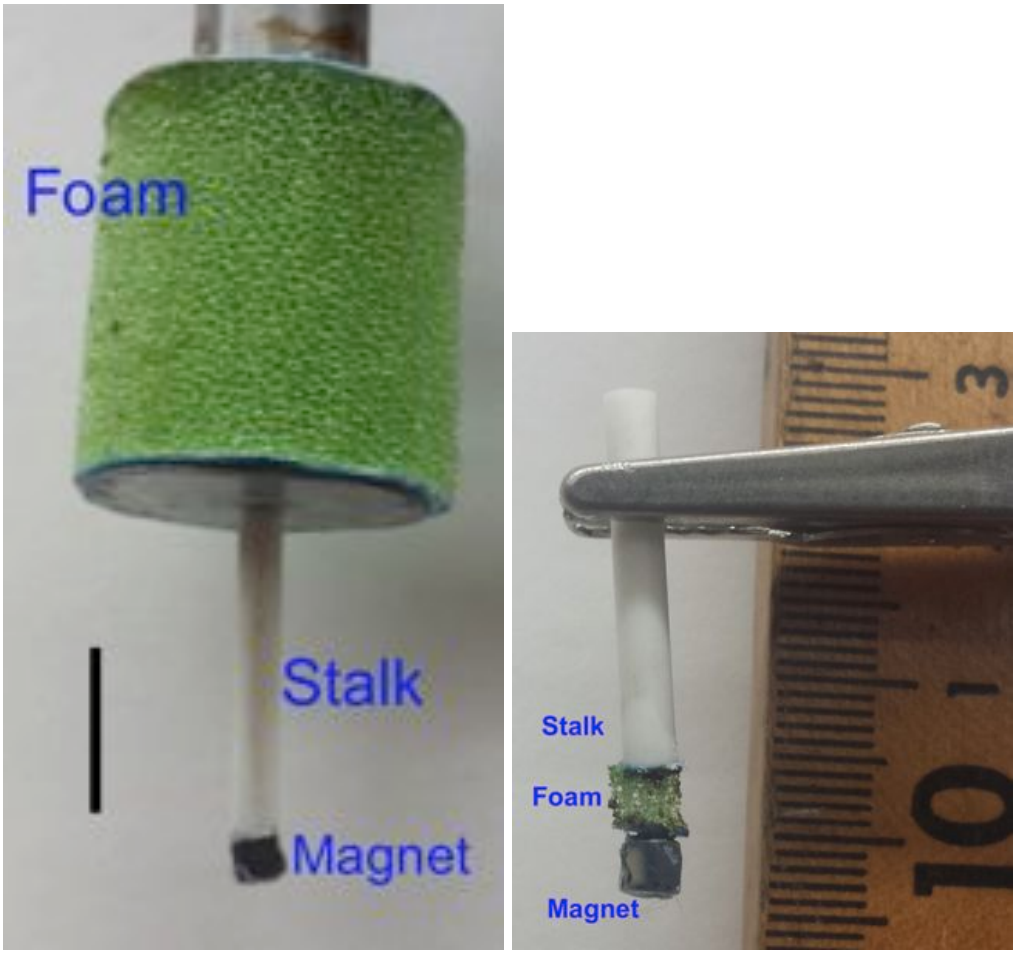

Figure 2: Specimens of foam with 0.4 mm cells. Left, larger specimen; scale bar 10 mm. Right, the smallest specimen; scale marks 1 mm.

during testing was less than 0.3%. This is well within the linear range of 5-10% for this sort of flexible foam. Linearity was also checked by conducting tests at different amplitude; moduli were independent of amplitude. Linear viscoelasticity was verified by observing the shape of the elliptic torque-angle curve, an elliptic Lissajous figure. The light detector was sufficiently sensitive that quality of the signals was good and the ratio of signal to noise was high, 40 to 400.

For bending, the light detector mode was switched to vertical detection and the beam calibration constant was determined accordingly; the driving signal was input to the orthogonal bending Helmholtz coil. A correction was applied to account for the additional bending moment imposed by the weight of the magnet and stalk; this correction was 3% or less. A correction was also applied to the effective specimen length to incorporate the effect of glue in the pores at the ends. The glue ingression was 0.3 mm or less per end. The correction was at most 10% for the smallest specimen of small cell foam and considerably less otherwise.

Compression tests were done to ascertain the behavior in the absence of macroscopic gradients of strain or rotation. This was done by applying force via dead weights on one end piece cemented to the specimen. The other end piece was cemented to a base upon an optical table. Deformation was measured using an LVDT; its stem was cemented to the upper end piece. The LVDT was

calibrated using a micrometer driven translation stage. The maximum strain achieved was 1.1%, well within the linear range for a flexible foam. A lower limit on specimen size was imposed by the tendency of small specimens to buckle.

Square section specimens of rubber and of foam with 0.4 mm cells were subjected to torsion with the aim of illustrating the effect of asymmetric stress in Cosserat elasticity. A small notch, about 1/15 the specimen width, was observed. In classical elasticity the notch will not displace because the symmetry of the stress implies zero stress, hence zero strain at the corner. In a Cosserat solid, the stress is asymmetric, so the notch can displace [17]; such displacement was observed in bone and dense foams [19].

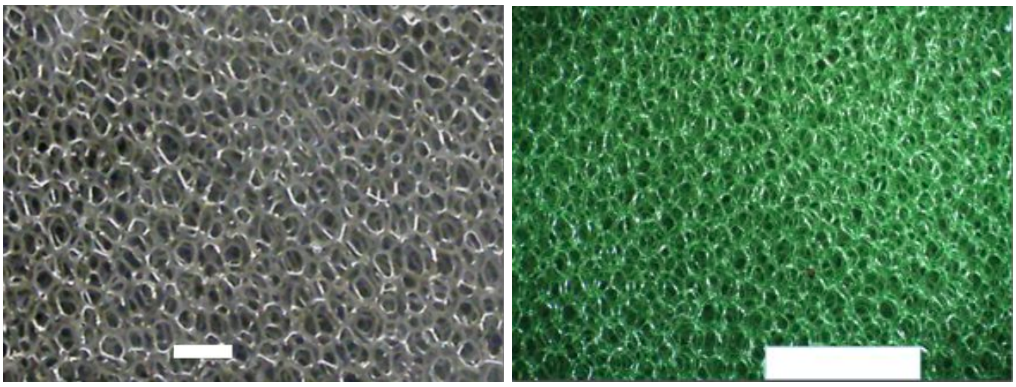

Figure 3: Open cell polyurethane foam. Left, larger cells; scale bar, 5 mm. Right, smaller cells; scale bar, 5 mm.

2.2 Analysis and interpretation

Size effect results were interpreted as follows. For torsion, the shear modulus G was found from the asymptote of rigidity vs. diameter curve for large size. The torsion characteristic length ℓ_t was found from fitting the points for the larger specimens to the following approximate solution. For torsion of a Cosserat elastic circular rod of radius r, ratio of structural rigidity to its classical counterpart (in the absence of gradient, for large diameter) is

$$\Omega = 1 + 6(\ell_t/r)^2. \tag{10}$$

This shows size effects to occur in torsion: slender specimens appear to have a higher effective modulus than thick ones. The classical torsional rigidity is $\frac{M}{\theta} = G[\frac{\pi}{2}r^4]$ so for Cosserat elasticity in this regime, $\frac{M}{\theta} = G[\frac{\pi}{2}r^4](1 + 6(\ell_t/r)^2)$. G is the true shear modulus in the absence of gradients; M is applied moment and θ is angular displacement. This expression is exact for $N = 1$; for other N the exact solution is more complicated and involves Bessel functions [7]:

$$\Omega = (1 + 6(\ell_t/r)^2)[\frac{(1 - 4\Psi\chi/3)}{1 - \Psi\chi}], \tag{11}$$

in which $\chi = I_1(pr)/prI_0(pr)$, $p^2 = 2\kappa/(\alpha + \beta + \gamma)$ and I_0 and I_1 are modified Bessel functions of the first kind.

The shear modulus G and characteristic length ℓ_t were determined by fitting experimental data for the three largest specimens to Eq. 10. The value of N was found by fitting Eq. 11 to the full data set using MATLAB. The curve is rather insensitive to Ψ except near the origin.

For bending, the classical bending rigidity is $\frac{M}{\theta} = E[\frac{\pi}{4}r^4]$. For bending of a Cosserat elastic circular rod and radius r, the rigidity ratio is approximately

$$\Omega = 1 + 8(\ell_b/r)^2 \frac{(1-(\beta/\gamma)^2)}{(1+\nu)}. \tag{12}$$

The expression is approximate for small characteristic length $\ell_b << r$. The exact form [8], which also involves Bessel functions, is

$$\Omega = 1 + 8(\ell_b/r)^2 \frac{(1-(\beta/\gamma)^2)}{(1+\nu)} + \frac{8N^2}{(1+\nu)}[\frac{(\beta/\gamma+\nu)^2}{\zeta(\delta a) + 8N^2(1-\nu)}] \tag{13}$$

with $\delta = N/\ell_b$ and $\zeta(\delta r) = (\delta r)^2[((\delta r)I_0((\delta r)) - I_1((\delta r)))/((\delta r)I_0(\delta r) - 2I_1(\delta r))]$.

The Young's modulus E and an initial value for the characteristic length ℓ_b were determined by fitting data for the three largest specimens to Eq. 12, with N input from the torsion analysis, $\beta/\gamma = 0.8$ based on prior dense foam and also from lattice analysis (see below), and ν from prior experimental results. Finally the values of ℓ_b and β/γ were found by fitting Eq. 13 to the full data set using MATLAB.

To obtain all six Cosserat constants, both torsion and bending experiments are required. The bend test provides some verification in that the shape of the size effect curve depends not only on E and ℓ_b but also on N and ℓ_t.

3 Results and discussion

3.1 Size effects and elastic constants

Density of foam specimens was independent of size to within a few percent. As for tests of anisotropy, the foam with 1.2 mm cells was anisotropic, with a ratio of compressive moduli in different directions of 1.6; the foam with 0.4 mm cells was isotropic to within 10%. Anisotropy was not obvious in images of foam observed from different directions.

Results of torsion size effect studies on the foam with 1.2 mm cells are shown in Figure 4. Also shown for comparison are theoretical curves for various N. Classical elasticity corresponds to a horizontal line with $\Omega = 1$.

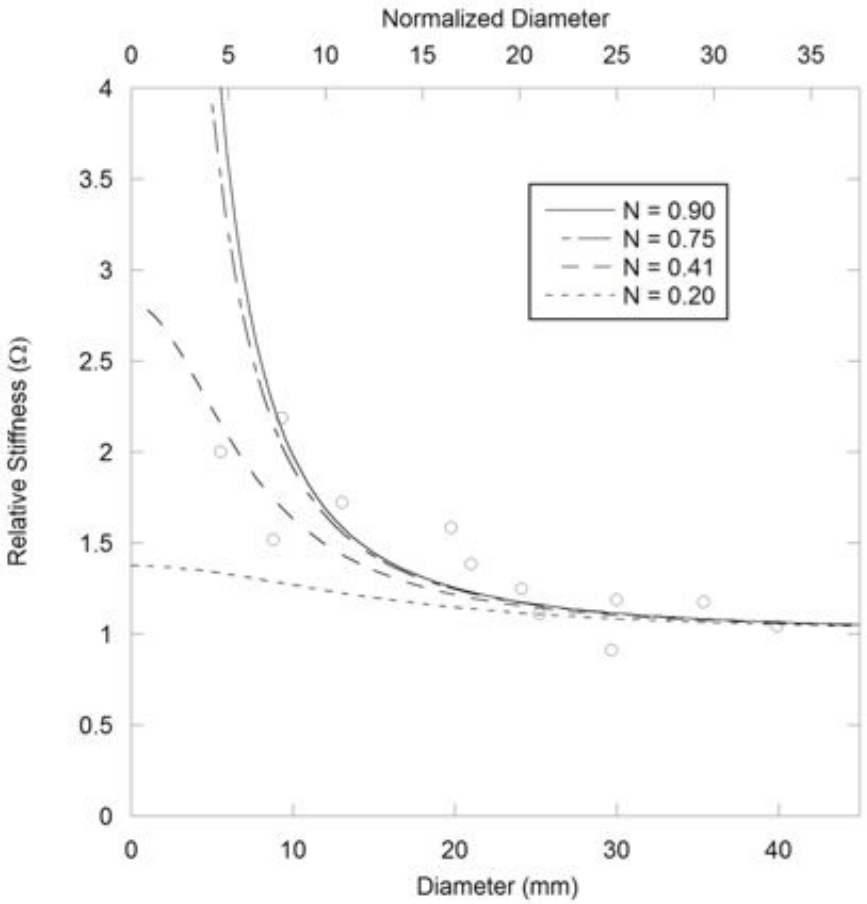

Figure 4: Size effects for foam with 1.2 mm cells in torsion. Top scale, diameter normalized to cell size. Open circles represent experimental results.

The torsion size effect curve for foam with 1.2 mm cells is consistent with $G = 45$ kPa, The characteristic length for torsion was $\ell_t = 2.1$ mm, $N = 0.41$, and $\Psi = 1.5$. The curve is rather insensitive to Ψ except near the origin.

The Poisson's ratio was determined [25] to be approximately 0.3. This value was also given by [1] as the mean of many measurements by various authors.

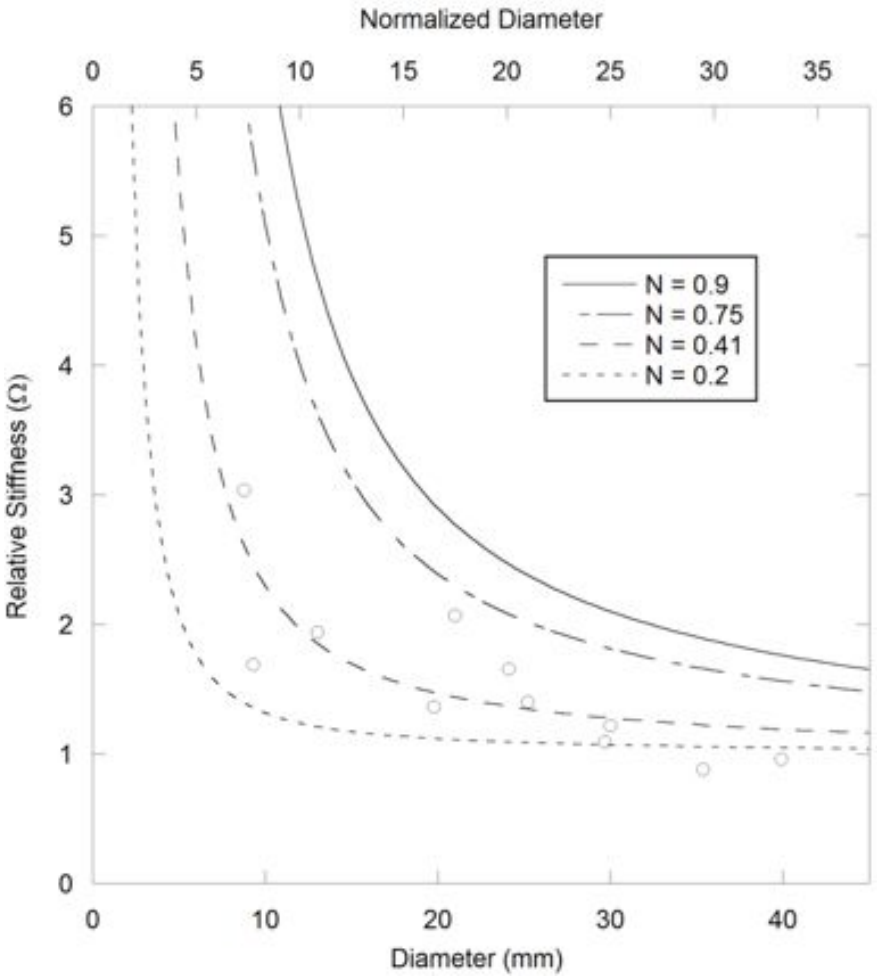

Figure 5: Size effects for foam with 1.2 mm cells in bending. Top scale, diameter normalized to cell size. Open circles represent experimental results.

Results of bending size effect studies on the foam with 1.2 mm cells are shown in Figure 5. As above, theoretical curves for various N are shown for comparison. The elastic constants obtained from the fit were $E = 91$ kPa, $\ell_b = 9$ mm, $\beta/\gamma = 0.83$. $N = 0.41$ was used based on torsion. This foam is anisotropic, so the characteristic length for bending is independent of the characteristic length for torsion and is independent of β/γ inferred from bending.

Results of torsion size effect studies on the foam with 0.4 mm cells are shown in Figure 6; results for bending are shown in Figure 7. Classical elasticity corresponds to a horizontal line with $\Omega = 1$. Inferred elastic constants are shear modulus $G = 28$ kPa, characteristic length for torsion $\ell_t = 1.6$ mm, $N = 0.99$, and $\Psi = 1.5$; Young's modulus $E = 81$ kPa, $\ell_b = 2.2$ mm, $\beta/\gamma = 0.8$. As a test of sensitivity, the point for the smallest specimen was omitted and another curve fit done; this resulted in $N = 0.82$; the mean square deviation between data and theoretical fit changed minimally by 5%.

Characteristic length values were larger for the larger cell foam as expected. The difference was, however, not directly proportional to the cell size. That is not surprising because the foams do not have identical structure; the foam with larger cells exhibited anisotropy. Too, surface tension during foam formation influences the details of the microstructure.

The inferred N was larger for the 0.4 mm cell foam: 0.99 vs. 0.41. The R^2 value as a measure of goodness of fit was compared for several values of N. For the 0.4 mm cell foam, $R^2 = 0.98$ for $N = 0.99$; 0.6 for $N = 0.6$. For the 1.2 mm cell foam, $R^2 = 0.65$ for $N = 0.41$; $R^2 = 0.4$ for $N = 0.3$ or 0.55. The difference in N is attributed to differences in the structure of the foams, especially the presence of incomplete cells in the 1.2 mm cell foam as discussed below.

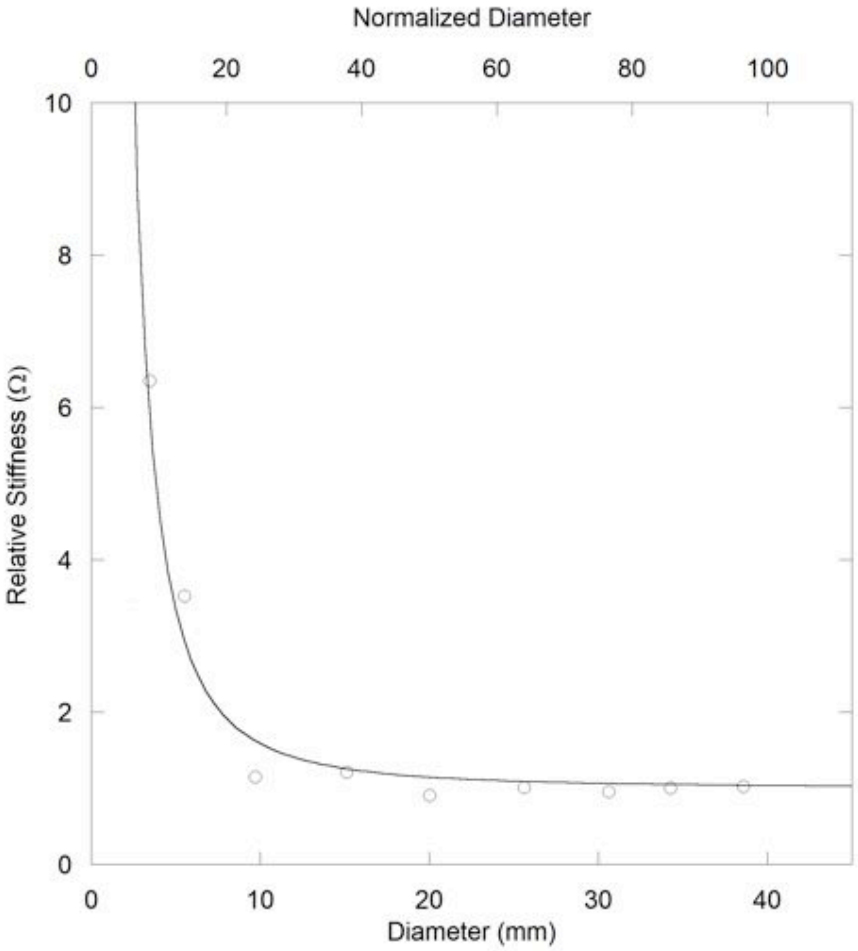

Figure 6: Size effects for foam with 0.4 mm cells in torsion. Top scale, diameter normalized to cell size. Open circles represent experimental results.

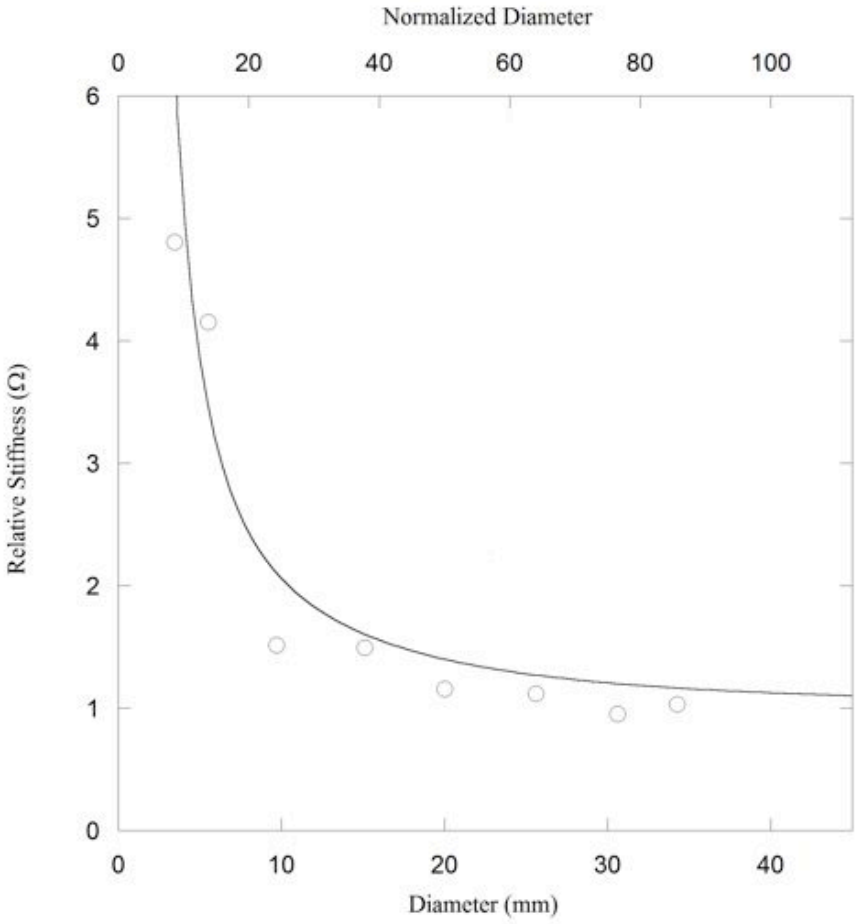

Figure 7: Size effects for foam with 0.4 mm cells in bending. Top scale, diameter normalized to cell size. Open circles represent experimental results.

Compression studies disclosed a modest softening size effect in which slender specimens have a smaller effective Young's modulus than thicker ones, Figure 8. Straight lines are least squares fits. This effect is opposite to the torsion and bending size effects observed and is opposite to the predictions of Cosserat elasticity. It is consistent with the notion of a surface layer of incomplete cells which do not fully contribute to the structural stiffness of the specimen.

A softening size effect is known to occur in foams as a result of damaged or incomplete cells at the surface [26] [14]. Softening size effects have also been observed in metal foams in compression and bending; these have been analyzed and attributed to strain localization [27]. Such localization can occur in foam at sufficiently high strain levels. Incomplete cells can also contribute to the fluctuation in effective stiffness with specimen size. Such fluctuation or scatter was observed to be considerably greater in the present low density open cell foams than it was for closed cell foams. Scatter was a result of material heterogeneity, not signal quality (which was good). Too, the low density foams may have heterogeneity on a scale larger than the cells. The effect of incomplete cells is for the effective modulus to becomes smaller as specimen size is reduced. This effect was observed in the compression studies in which average stress is constant and there is no contribution from Cosserat or other gradient related effect. The effect of incomplete cells in the bending and torsion studies is to reduce the inferred Cosserat constants, so the intrinsic Cosserat elastic constants will

be even larger than those reported.

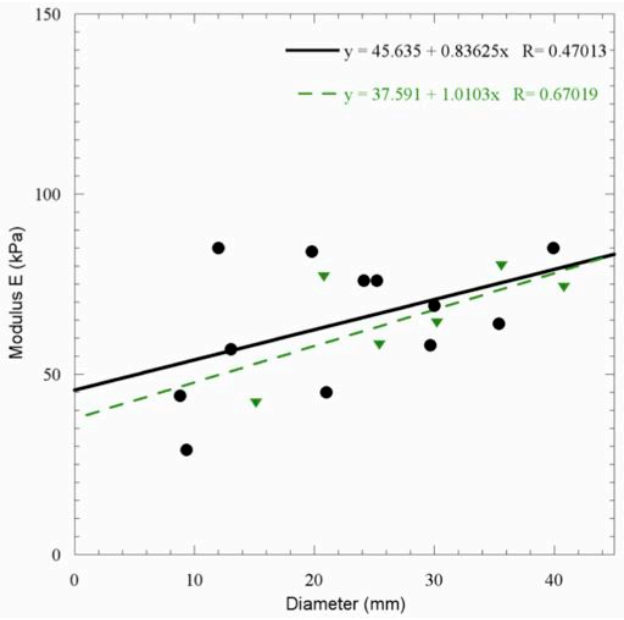

Figure 8: Young's Modulus of foam in compression; circles, foam with 1.2 mm cells; triangles, foam with 0.4 mm cells.

3.2 Viscoelastic damping

Viscoelastic response, was determined as mechanical damping tan δ at 1 Hz. Because the same frequency was used for all experiments, viscoelastic dispersion (frequency dependence of modulus) cannot obtrude in the results or their interpretation. Damping of 1.2 mm cell foam was essentially independent of specimen size, as shown in Figure 9. Straight lines are least squares fits. The foam with smaller cells (Figure 10) also exhibited damping independent of size. So the Cosserat effects entail viscoelasticity but there is no size dependence of the damping. This is in contrast with the behavior of bone [28] which behaves as a Cosserat solid [15]. Size effects of large magnitude were observed in the torsional effective shear modulus and damping of bovine plexiform bone. Damping increased and stiffness decreased with bone specimen size. Bone in contrast to foam has heterogeneity with spatially varying viscoelastic response, specifically there are highly viscoelastic boundaries called cement lines between large fibers (osteons) in the bone [29]. As for the present foams, the difference in the overall damping of the two foams suggests a difference in chemical composition or density of cross links. From the foam density and modulus, The Young's modulus E_s of the solid material of which the foam is made is calculated from the classic Gibson-Ashby [1] relation $\frac{E}{E_s} = C_f[\frac{\rho}{\rho_s}]^2$ between rib modulus E_s and foam modulus E in which ρ_s is the density, C_f is a constant of value near one. For both foams, the rib Young's modulus is about 90 MPa, well into the transition or leathery regime for a polymer. The relatively large tan δ is understandable in that context.

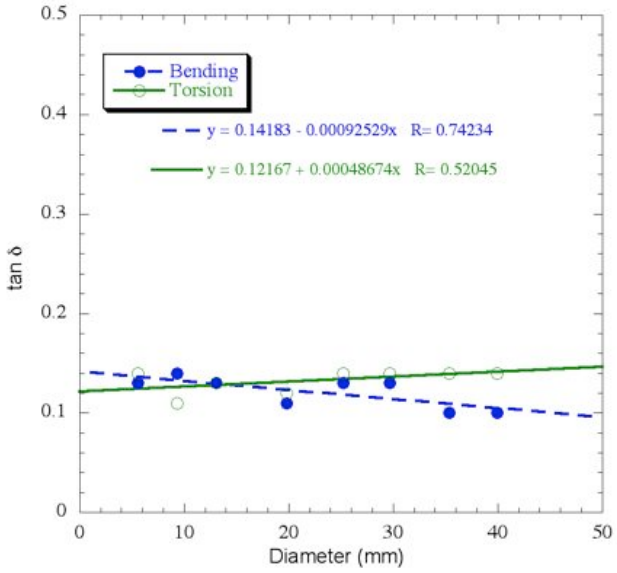

Figure 9: Viscoelastic tan δ vs. specimen size for foam with 1.2 mm cells. Solid symbols and dash line fit: bending. Open symbols and solid line fit: torsion.

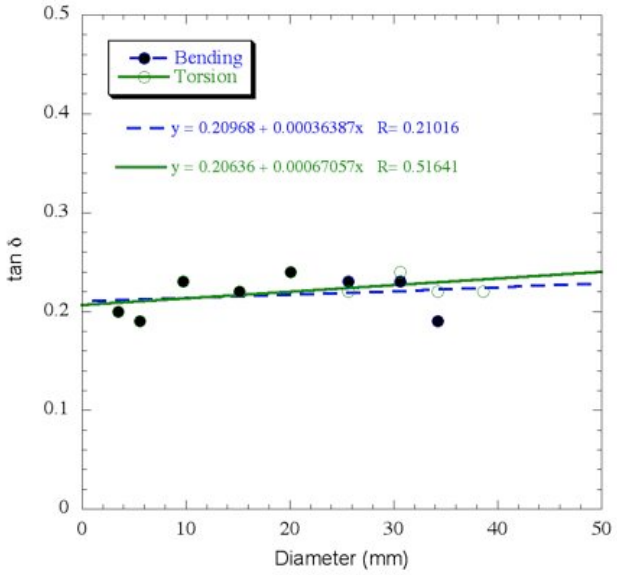

Figure 10: Viscoelastic tan δ vs. specimen size for foam with 0.4 mm cells.Solid symbols and dash line fit: bending. Open symbols and solid line fit: torsion.

3.3 Comparison with homogenization

Results show large characteristic lengths considerably larger than the cell size and large values of N. Comparison with homogenization analyses and with other experiment is of interest.

Lattices with straight ribs have analyzed as Cosserat continua [30] [31] [32]; homogenization such as long wave approximation reveals similarity to the Cosserat equations [30]. For cubical closed cells

with thin walls [32], $\ell = h/2\sqrt{3}$ is considerably smaller than the cell size h. These lattices are stretch dominated: the effective Young's modulus of the lattice is governed by stretching or compression of the ribs or plates comprising the lattice. Cosserat effects depend on bending or twisting of the ribs. If the ribs are slender, bending or twisting moments in them decrease more rapidly than axial forces, so Cosserat effects are weak. Analysis of two dimensional chiral honeycomb lattice structures as Cosserat continua reveals bend dominated behavior in which Young's modulus is governed by rib bending. These honeycombs have large N approaching its upper bound 1, and characteristic length ℓ comparable to the cell size [33]. The ribs of this lattice are bend dominated is in contrast to prior stretch dominated lattices that have been analyzed thus far [35] [36] [37], in which slender ribs correspond to small N and small ℓ. In summary, the large N and ℓ values in these materials is understandable in the context of the role of bending and torsion of the cell ribs.

3.4 Comparison with other experiment

As for comparison with other experiment, prior dense closed cell foams [13], [14] studied experimentally had a relatively small $N = 0.2$, hence comparatively weak size effects. The maximum size effect ratio Ω was 1.3 for dense polyurethane foam and 1.44 for Rohacell foam, much smaller than in the present foams. Foam [14] with comparatively uniform closed cell size had ℓ comparable to the cell size. Foam [13] with substantial heterogeneity of closed cell size had ℓ larger than the cell size. The structures differ considerably from that of the low density open cell foams examined here, which are about one tenth the density of the prior foams. Recently it was shown that classical continuum theories, such as Bernoulli-Euler beam theory, are inadequate for describing the elastic bending behavior of metal foams [38]. Some cell models were developed for analysis. While such models show the physical origin of the local moments that we interpret via Cosserat elasticity, they have not been couched in such a way to anticipate effects in torsion or changes in strain distribution as is possible with a generalized continuum approach such as Cosserat elasticity. Large characteristic lengths, larger than the cell size are consistent with observations of sigmoid curvature of the lateral surfaces of bent square cross section bars and analysis via Cosserat elasticity [34]. Experimental observation of this sigmoid curvature is consistent too with a large positive value of β/γ. A value β/γ between 0.5 and 1 is sensible based on post-processing of the results of [31], who performed homogenization analysis of a 3-D cubic lattice of straight ribs. No known Cosserat models are available to predict elastic constants for foam.

3.5 Asymmetry of the stress

Asymmetry of the stress was inferred from displacement of a notch at the corner of a square cross section bar in torsion. Displacement was observed in foam with 0.4 mm cells but not in rubber which is classical on a macroscopic scale (Figure 11). Displacement of the corner notch cannot occur in classically elastic solids because the symmetry of the stress implies stress, hence strain, are zero at the corner. Generalized continuum theories that entail symmetry of the stress also predict zero motion of the notch. The foam exhibits such a displacement in contrast with rubber. So the foam has Cosserat degrees of freedom independent of other freedom associated with generalized continuum theories.

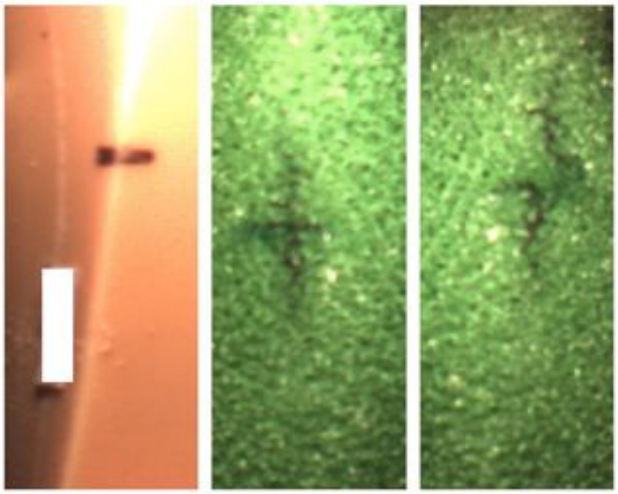

Figure 11: Corner of rectangular section bars, with notch marked in black ink. Left, twisted rubber; scale bar, 5 mm. Center, foam, 0.4 mm cells, not twisted. Right, foam, 0.4 mm cells, twisted.

3.6 Generalized continuum theories

A variety of continuum theories can be used to interpret experiments. We consider it to be sensible to use the simplest one that incorporates known physics of the material and that is consistent with experiment. A substantial material size scale does not guarantee the material exhibits generalized continuum properties. For example a composite containing beads of aluminum in a polymer matrix behaved classically in size effect studies [7]; a syntactic foam containing hollow glass spheres was also essentially classical [13] in contrast to dense polyurethane foam which was Cosserat. The present experimental results show size effects that do not occur in classically elastic materials. They are interpreted in the context of Cosserat elasticity which has more freedom than classical elasticity and allows for size effects. Also, Cosserat elasticity incorporates local rotation and distributed moments. These variables are incorporated in classical analyses [1] of foams in compression to determine moduli; there are no gradients of rotation in that case. As for variants of the Cosserat continuum, the smaller cell foam has a large value of $N = 0.99$. This may be regarded as consistent with $N = 1$, corresponding the the special case of Cosserat elasticity called couple stress elasticity [11]. The larger cell foam has a smaller N, not consistent with $N = 1$.

As for the possibility of additional freedom, observe that the definitions of characteristic lengths, Eq. 6, 7 entail a relation between ℓ_t, ℓ_b, and β/γ for isotropic materials. Based on this relation, ℓ_b is larger than expected by a factor of about 2.5. Results do not necessarily exclude the presence of additional freedom such as that incorporated in micromorphic / Mindlin microstructure [12] theory. Micromorphic elasticity includes the freedom of Cosserat elasticity as well as the freedom of the microstructure to deform as well as translate and rotate; it requires 18 elastic constants for an isotropic material. Microstretch elasticity [39] is a subset of microstructure elasticity that incorporates the freedom of Cosserat elasticity as well as sensitivity to gradient of local dilatation. Sensitivity to dilatation gradient of voids [6] when considered alone, gives rise to size effects in bending but not in torsion. Such a theory cannot account for the observed size effects in any of the foams studied, including the present ones. Microstretch elasticity, which includes sensitivity to gradients of rotation and of dilatation could account for bending effects larger than those of Cosserat elasticity. In bending or compression, the dilatational component of deformation can be

expected to cause dilation of individual cells, otherwise the bulk modulus would diverge. Indeed, local dilation [40] was observed in cells of metal foam in compression. Theoretical framework is not, however, available to determine dilatation sensitivity independently of rotation sensitivity. A highly simplified plasticity model based on micromorphic theory was used to study stress concentration effects in metal foam [42]. A characteristic length for plasticity was determined. This is in contrast to the present experiments which deal with small strain elasticity and viscoelasticity, and with inference of all the Cosserat elastic constants. As for elasticity, there is no known analytical solution by which to interpret size effects via micromorphic elasticity theory.

Generalized continuum freedom can also be explored via waves. Indeed, dispersion of longitudinal waves and cut-off frequencies were observed in foams of the type studied here [41]. In a micro-structural view, the wave effects were attributed to micro-vibrations of the cell ribs in a structural view. In a generalized continuum view, the effects were associated with microstructure / micromorphic elasticity; Cosserat elasticity predicts dispersion of shear waves but not longitudinal waves.

In summary, substantial Cosserat effects do occur in these foams. Effects of dilatation gradient cannot contribute to observed size effects in torsion; they may contribute to size effects in bending. As for the determination of all the 9 elastic constants of a microstretch model or all the 18 constants of a micromorphic model, the requisite exact analytical solutions for interpretation of experiments are not yet available.

4 Conclusions

Large size effects are observed in the torsion and bending of reticulated open cell polymer foams. These effects are inconsistent with classical elasticity but can be modeled with Cosserat elasticity.

5 Acknowledgements

We gratefully acknowledge support of this research by the National Science Foundation via Grant CMMI-1361832.

References

[1] Gibson, L. J. and Ashby, M. F., *Cellular Solids*, Pergamon, Oxford; 2nd Ed., Cambridge (1997).

[2] Cosserat, E. and Cosserat, F., *Theorie des Corps Deformables*, Hermann et Fils, Paris (1909).

[3] Mindlin, R. D., Stress functions for a Cosserat continuum, Int. J. Solids Structures, **1**, 265-271 (1965).

[4] Eringen, A. C., 1968, Theory of micropolar elasticity. In *Fracture*, **1**, 621-729 (edited by H. Liebowitz), Academic Press, NY.

[5] Ilcewicz, L., Kennedy, T. C., and Shaar, C., Experimental application of a generalized continuum model to nondestructive testing, J. Materials Science Letters **4**, 434-438 (1985).

[6] Cowin, S. C. and Nunziato, J. W., Linear elastic materials with voids, J. Elasticity **13** 125-147 (1983).

[7] Gauthier, R. D. and W. E. Jahsman, A quest for micropolar elastic constants. J. Applied Mechanics, **42**, 369-374 (1975).

[8] Krishna Reddy, G. V. and Venkatasubramanian, N. K., On the flexural rigidity of a micropolar elastic circular cylinder, J. Applied Mechanics **45**, 429-431 (1978).

[9] Mindlin, R. D., Effect of couple stresses on stress concentrations, Experimental Mechanics, **3**, 1-7, (1963).

[10] Timoshenko, S.P., *History of Strength of Materials*, Dover, NY, 1983.

[11] Koiter, W. T., Couple-Stresses in the theory of elasticity, Parts I and II, Proc. Koninklijke Ned. Akad. Wetenshappen **67**, 17-44 (1964).

[12] Mindlin, R. D., Micro-structure in linear elasticity, Arch. Rational Mech. Analy, **16**, 51-78, (1964).

[13] Lakes, R. S., Experimental microelasticity of two porous solids, Int. J. Solids and Structures, **22**, 55-63 (1986).

[14] Anderson, W. B. and Lakes, R. S., Size effects due to Cosserat elasticity and surface damage in closed-cell polymethacrylimide foam, J. Materials Science, **29**, 6413-6419 (1994).

[15] Lakes, R. S., On the torsional properties of single osteons, J. Biomechanics, **28**, 1409-1410 (1995).

[16] Mora, R. and Waas, A. M., Measurement of the Cosserat constant of circular cell polycarbonate honeycomb, Philosophical Magazine A, **80**, 1699-1713 (2000).

[17] Park, H. C. and R. S. Lakes, Torsion of a micropolar elastic prism of square cross section. Int. J. Solids, Structures, **23**, 485-503 (1987).

[18] Park, H. C. and Lakes, R. S., Cosserat micromechanics of human bone: strain redistribution by a hydration-sensitive constituent, J. Biomechanics, **19**, 385-397 (1986).

[19] Lakes, R. S., Gorman, D., and Bonfield, W., Holographic screening method for microelastic solids, J. Materials Science, **20**, 2882-2888 (1985).

[20] Anderson, W. B., Lakes, R. S., and Smith, M. C., Holographic evaluation of warp in the torsion of a bar of cellular solid, Cellular Polymers, **14**, 1-13 (1995).

[21] Nyilas, R. D., Kobas, M., Spolenak, R., Synchrotron X-ray microdiffraction reveals rotational plastic deformation mechanisms in polycrystalline thin films, Acta Materialia **57**: 3738-3753 (2009).

[22] Foamade Industries, Auburn Hills, MI.

[23] Brodt, M., Cook, L. S., and Lakes, R. S., Apparatus for determining the properties of materials over ten decades of frequency and time: refinements, Rev. Sci. Instrum. **66**, 5292-5297, (1995).

[24] Lee, T. Lakes, R. S., and Lal, A. Resonant ultrasound spectroscopy for measurement of mechanical damping: comparison with broadband viscoelastic spectroscopy, Rev. Sci. Instrum., **71**, 2855-2861, (2000).

[25] Wang, Y. C., Lakes, R. S., and Butenhoff, A., Influence of cell size on re-entrant transformation of negative Poisson's ratio reticulated polyurethane foams, Cellular Polymers, **20**, 373-385 (2001).

[26] Brezny, R. and Green, D. J. Characterization of edge effects in cellular materials J. Materials Science, **25** (11), 4571-4578 (1990)

[27] C. Tekoglu, L.J. Gibson, T. Pardoen, P.R. Onck Size effects in foams: Experiments and modeling, Progress in Materials Science **56**, 109-138, (2011).

[28] Buechner, P. M., and Lakes, R. S., Size effects in the elasticity and viscoelasticity of bone, Biomechanics and Modeling in Mechanobiology, **1** (4), 295-301 (2003).

[29] Lakes, R. S. and Saha, S., Cement line motion in bone, Science, **204**, 501-503 (1979).

[30] Askar, A. and Cakmak, A. S. A structural model of a micropolar continuum, Int. J. Engng. Sci. **6**, 583-589, (1968).

[31] Tauchert, T., A lattice theory for representation of thermoelastic composite materials, Recent Advances in Engineering Science, **5**, 325-345 (1970).

[32] Adomeit, G., Determination of elastic constants of a structured material, Mechanics of Generalized Continua, (Edited by Kröner, E.), IUTAM Symposium, Freudenstadt, Stuttgart. Springer, Berlin (1967).

[33] Spadoni, A. and Ruzzene, M., Elasto-static micropolar behavior of a chiral auxetic lattice, J. Mechs Physics of Solids, **60**, 156-171 (2012).

[34] Lakes, R. S. and Drugan, W. J., Bending of a Cosserat elastic bar of square cross section - theory and experiment, J. Applied Mechanics, **82** (9), 091002 (2015).

[35] Banks, C.B., Sokolowski, M. On certain two-dimensional applications of the couple stress theory. Int. J. Solids Struct. **4** (1), 15-29 (1968).

[36] Wang, A.J., McDowell, D.L.. In-plane stiffness and yield strength of periodic metal honeycombs. J. Eng. Mater. Trans. ASME **126**, 137-156 (2004).

[37] Dos Reis, F., Ganghoffer, J.F., Construction of Micropolar Continua from the Homogenization of Repetitive Planar Lattices in *Mechanics of Generalized Continua, Advanced Structured Materials* Ed. Altenbach, H. Maugin, G., Erofeev, V., Springer, Volume 7 193-217 (Chapter 9) (2011).

[38] Triawan, F., Kishimoto, K., Adachi, T., Inaba, K. , Nakamura, T., Hashimura, T., The elastic behavior of aluminum alloy foam under uniaxial loading and bending conditions, Acta Materialia **60** 3084-3093 (2012).

[39] Eringen, A. C., Theory of thermo-microstretch elastic solids, Int. J. Engng. Sci., **28** (12)1291-1301, (1990).

[40] Burteau, A., NGuyen, F., Bartout, J.D., Forest, S., Bienvenu, Y., Saberi, S. and Naumann, D., Impact of material processing and deformation on cell morphology and mechanical behavior of polyurethane and nickel foams, International Journal of Solids and Structures, **49**, 2714-2732, (2012).

[41] Chen, C. P. and Lakes, R. S., Dynamic wave dispersion and loss properties of conventional and negative Poisson's ratio polymeric cellular materials, Cellular Polymers, **8** (5), 343-359 (1989).

[42] T. Dillard, S. Forest and P. Ienny, Micromorphic continuum modelling of the deformation and fracture behaviour of nickel foams, European Journal of Mechanics A, Solids, **25**, 526-549, (2006).